Supplementary Material for "Introducing a Low-Cost Approach for Environmental Monitoring with the Civil Air Patrol (CAP) Aircraft: An Example Addressing Greenhouse Gas Emissions"

Edward J. Strobach[1], Elaine Jaross[2], Xinrong Ren[3], Joel Dreessen[4], Paul Walter[5], James S. Wang[4], Maurice Roots[6,7], Julia Famiglietti[2], Austin Turner[2], Phillip Stratton[1,3], Russell R. Dickerson[1,8], Kenneth J. Davis[9,10], and Daniel P. Lathrop[2,11]

[1]Atmospheric and Oceanic Sciences Department, University of Maryland, College Park, MD 20742, USA
[2]Department of Geology, University of Maryland, College Park, MD 20742, USA
[3]NOAA Air Resources Laboratory, College Park, MD 20740, USA
[4]Maryland Department of the Environment, Baltimore, MD 21230, USA
[5]St. Edward's University, Austin, TX 78704, USA
[6]Atmospheric Physics, University of Maryland Baltimore County, Baltimore, MD 21250, USA
[7]NASA Goddard Space Flight Center, Greenbelt, MD 20771, USA
[8]Department of Chemistry, University of Maryland, College Park, MD 20742, USA
[9]Department of Meteorology and Atmospheric Science, Pennsylvania State University, University Park, PA 16802, USA
[10]Earth and Environmental Systems Institute, Pennsylvania State University, University Park, PA 16802, USA
[11]Department of Physics, University of Maryland, College Park, MD 20742, USA

Correspondence: Edward J. Strobach (estrobac@umd.edu)

Abstract. Research aircraft provide essential information about weather, climate forcing, and air quality (AQ). Instrumenting and deploying these aircraft, however, requires substantial investment. Single engine Cessna aircraft flown by the Civil Air Patrol (CAP) offer practical, economical, and widely available platforms for tropospheric sounding of meteorological variables, greenhouse gases (GHGs), and short-lived pollutants. A recent partnership with CAP has led to frequent surveys across the state of Maryland with a Licor 7810 to measure CO_2, CH_4, and H_2O concentrations for GHG analyses and a basic meteorological measurement suite to investigate transport and calculate emission rates (ERs) using the mass balance approach (MBA). The flexibility of multiple aircraft and pilots facilitates aerial surveys at weekly to bi-weekly timescales.

This paper outlines the steps required for a successful operation with the CAP, including flight planning and procedures, instrument calibration, and post-processing. Greenhouse gas emissions are used throughout as a worked example of what the platform can deliver, while the approach itself is general and extends to other areas of environmental monitoring. Examples of CAP flights highlight the strategic targeting of GHG emissions from sources selected through close coordination with the Maryland Department of the Environment (MDE), including frequent visits to facilities to quantify short-term variability of ERs. The documentation of frequent flights from this work and the availability of CAP aircraft in all 50 states demonstrates a scalable solution for frequent spatiotemporal GHG monitoring that addresses anthropogenic impacts, complements regional measurement efforts, and serves as a viable option for validating satellite retrievals.

1 Supplementary Material

This section contains additional figures and tables cited in the manuscript that support statements or conclusions made.

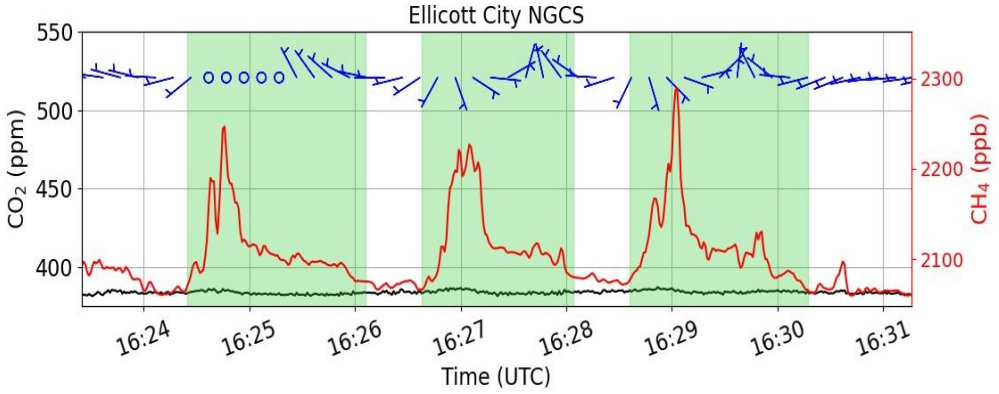

Figure S1. CO_2 (black), CH_4 (red), and wind barbs (blue) during survey of the Ellicott City NGCS on 8 January 2026. Green shading indicates the segments of data that overlap with the plume isolated. Notice the winds rotate with time which matches the spiral patterns shown in Figure 7.

Table S1 relies on calculations of biases and the root-mean-square error (RMSE) between flight-level winds and one of the CoURAGE DLs (i.e., S2, M1, and S3). The equation for bias follows

$$B(t_i \pm \Delta t/2, z_k \pm \Delta z/2) = CAP(t_i \pm \Delta t/2, z_k \pm \Delta z/2) - DL_{i,k} \tag{S1}$$

where biases (B) are calculated for all CAP measurements grouped with a DL profile at time, t_i, and height, z_k, i.e., $CAP(t_i \pm \Delta t/2, z_k \pm \Delta z/2) - DL_{i,k}$. The number of CAP measurements grouped for each time and height depends on how long and at what heights the aircraft flew when within 30 km of a DL. For calculations shown in Table S1, we averaged across both time and altitude to report a bulk estimate of biases for u, v, WS, and WD.

RMSE is calculated as follows

$$R = \left(\frac{\sum_{k=1}^{M} \left(\frac{\sum_{i=1}^{N} (CAP(t_i \pm \Delta t/2, z_k \pm \Delta z/2) - DL_{i,k})^2}{N} \right)}{M} \right)^{\frac{1}{2}} \tag{S2}$$

where the argument in Equation S2 is the bias-squared averaged over all instances in time for each height followed by an average across the vertical. Both Equations S1 and S2 are reported in Table S1.

Table S1. CAP flight vs. Doppler Lidar wind comparison statistics. Bias = flight − lidar. Units: m s^{-1} for u, v, WS; degrees for WD. Sites: S2 (Beltsville), M1 (Baltimore), S3 (Kent Island). Flight measurements are only considered within 30 km of DLs. There are instances where we did not fly within 30 km of these sites; those are indicated by dashes. Flight-level winds are grouped for each DL profile where there is temporal overlap, where Δt represents the time between DL measurements and $t_i \pm \Delta t/2$ represents the time window centered on a DL measurement, t_i. Winds are also grouped for each measurement height of the DL, where Δz in this case represents the vertical resolution of the DL and $z_k \pm \Delta z/2$ represents the height range of CAP measurements centered at a measurement height, z_k, across the length of the DL range gate, [$-\Delta z/2, \Delta z/2$]. CAP flight winds grouped for each DL measurement time and height bin are used to calculate biases and root-mean-square error (RMSE) as shown below. Differences are calculated as flight winds - DL. Equations S1 and S2 represent the bias (B) and root-mean-squared error (RMSE–R) calculations for u, v, WS (wind speed), and WD (wind direction) averaged across time and height. A circular difference and mean is applied to wind direction. While plenty of cases show small biases and RMSE, there are clearly cases with very large biases and RMSE. Considering the use of DL for the cases where large differences are observed would further add uncertainty to calculations of ERs in Section 5. Rather than choosing only the days where there was good agreement, we instead rely only on flight level winds to maintain consistency across all days.

	S2								**M1**								**S3**							
	u		v		WS		WD		u		v		WS		WD		u		v		WS		WD	
Date	B	R	B	R	B	R	B	R	B	R	B	R	B	R	B	R	B	R	B	R	B	R	B	R
2025-02-24	1.1	1.5	-1.2	1.4	0.0	0.5	-38	112	-5.1	5.5	6.1	6.9	3.0	3.6	-90	93	1.5	2.2	4.7	5.1	5.1	5.3	3	12
2025-03-03	–	–	–	–	–	–	–	–	5.2	6.2	2.1	2.7	0.4	2.0	14	136	1.7	2.6	1.5	2.1	1.9	2.7	-21	30
2025-03-19	1.0	1.9	7.8	8.5	6.7	7.6	19	33	-6.8	7.7	0.3	3.6	0.5	2.8	-98	100	–	–	–	–	–	–	–	–
2025-07-02	–	–	–	–	–	–	–	–	-2.1	2.4	-1.4	1.6	-1.9	2.0	22	74	1.4	2.1	-0.5	1.1	1.1	1.7	-12	87
2025-07-08	-0.3	1.9	1.3	1.9	0.2	1.8	-10	23	–	–	–	–	–	–	–	–	–	–	–	–	–	–	–	–
2025-07-14	-0.8	1.5	2.7	2.8	2.7	2.9	-23	44	0.0	1.0	0.9	1.2	0.8	1.2	3	16	1.8	2.0	0.1	0.5	0.4	0.6	31	33
2025-07-23	-0.4	1.2	2.9	3.1	2.7	3.0	5	31	0.7	1.7	2.9	3.1	1.9	2.4	36	42	–	–	–	–	–	–	–	–
2025-07-29	–	–	–	–	–	–	–	–	1.0	1.8	-1.2	2.4	0.4	1.4	43	100	0.4	1.2	0.3	1.5	0.8	1.4	10	70
2025-08-15	-1.8	2.9	-0.8	1.4	0.8	1.7	-53	88	0.2	1.6	-0.5	1.6	0.0	1.5	-8	38	0.3	1.2	0.6	1.0	-0.3	1.3	9	16
2025-10-28	-1.4	2.5	-3.1	3.6	2.3	2.9	-18	24	-1.0	2.4	-2.7	3.0	2.2	3.0	-11	14	–	–	–	–	–	–	–	–

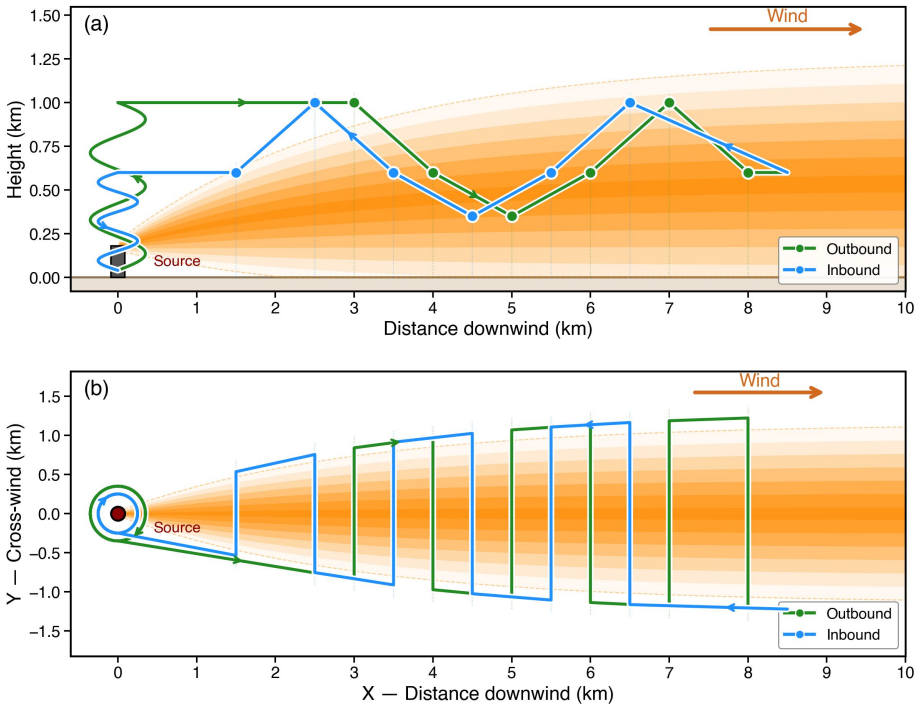

Figure S2. Idealized schematic of the combined lawnmower and sawtooth flight pattern used to fill a downwind volume, shown for a plume advected to the right by the wind. a) The vertical sawtooth viewed in the along-wind plane, with the aircraft climbing and descending between ≈0.35 km and 1 km as it works downwind of the source. b) The horizontal lawnmower viewed from above, with successive crosswind legs widening as the plume disperses. Outbound (green) and inbound (blue) portions of the pattern are offset from one another so that the interleaved passes sample the plume twice. Orange shading indicates the plume, with the dashed lines marking its nominal edges. The tight spiral at the source in both panels represents the initial climb. This pattern is the alternative to the spirals of Section 2.4 and produces the wall sampled in Figure 6.

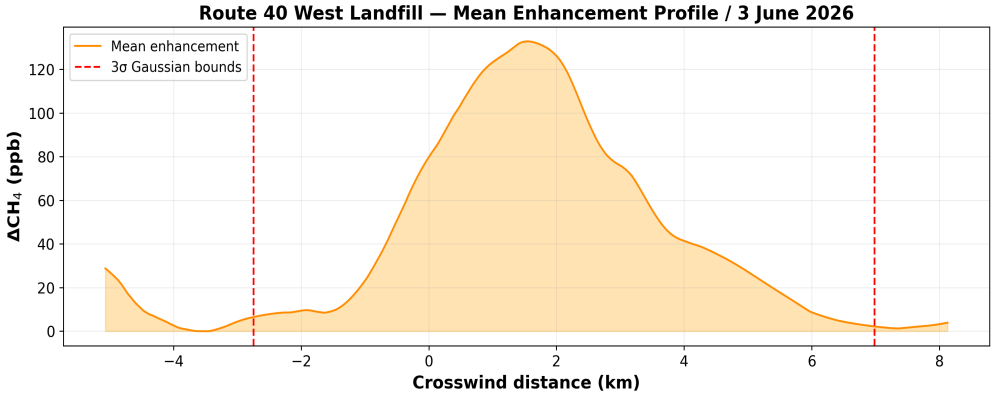

Figure S3. Mean CH_4 enhancement profile (orange) across the downwind wall sampled over the Route 40 West landfill on 3 June 2026, obtained by averaging the kriged enhancement field of Figure 6d over altitude. Red dashed lines mark the $\pm 3\sigma$ bounds of a Gaussian fit to the profile, which set the crosswind limits of integration used in the volumetric mass balance described in Section 4.3. Enhancements outside these bounds remain small relative to the peak, supporting the choice of background.

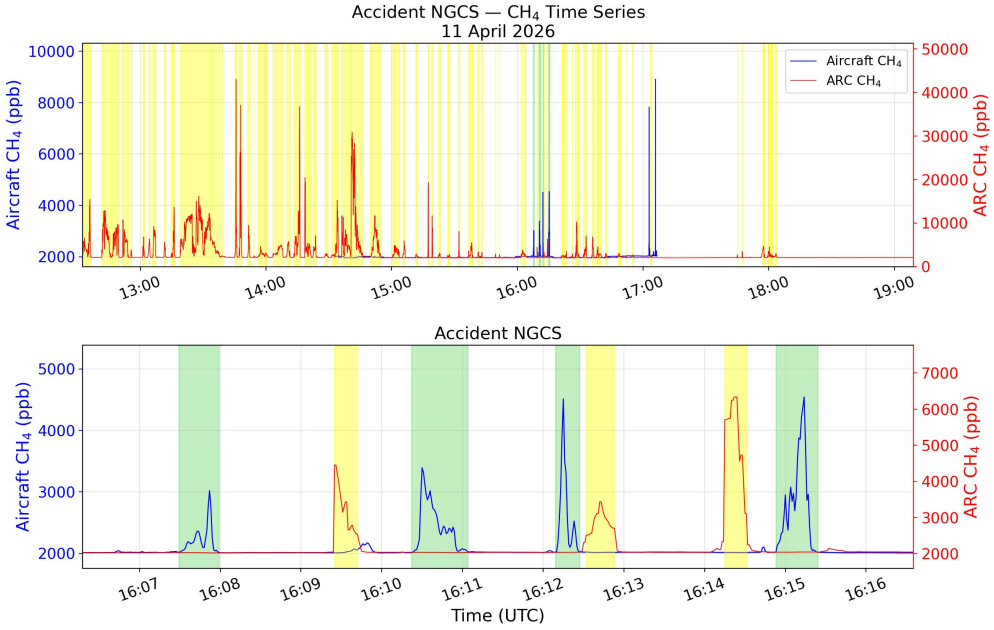

Figure S4. CH_4 time series from the CAP aircraft (blue, left axis) and NOAA's Air Resources Car (ARC; red, right axis) during coordinated sampling near the Accident NGCS on 11 April 2026. a) The full period of overlap between 12:30 and 19:00 UTC, with yellow shading marking ARC plume intercepts and green shading marking CAP plume intercepts. b) A zoom-in on 16:06–16:16 UTC, when both platforms repeatedly intercepted the plume within the same few minutes. Note that the two axes span very different ranges in both panels, and that the ranges differ between a) and b).